Photonic Bandgap of Random in Layer Position Extrinsic Magnetized Plasma Multilayer

Chittaranjan Nayak, Carlos H. Costa, and Kanaparthi V. Phani Kumar

***Abstract*— The transmittance of electromagnetic waves, with normal incidence, in 1-D random extrinsic magnetized plasma photonic structures is studied numerically based on the transfer-matrix method. Here, the homogeneous magnetized plasma having a uniform density profile is considered. Continuing a previous study [IEEE T. Plasma Sci., vol. 47, no. 4, pp. 1726–1733, 2019], we investigate how the main photonic bandgap in an extrinsic magnetized plasma photonic structure changes when the positions of the layers in the entire structure are random. The numerical calculations show that a robust photonic bandgap can be realized up to a certain probability of occurrence. Also, we show that the proposed random multilayered structure can work as a robust tunable photonic lattice which can be controlled by the plasma parameters and the external magnetic field.**

***Index Terms*— Electromagnetic propagation in plasma media, electromagnetic propagation in random media, multilayered media, photonic bandgap materials, spectral analysis.**

I. Introduction

PHOTONIC crystals (PCs), which are materials that can model and control the light propagation by the emergence of the photonic bandgaps, were presented by Yablonovith [1] and John [2] independently in 1987. Since then, PCs have attracted the attention of many theoretical and experimental research groups around the world and which has conducted several investigations to develop the next generation of the technological devices based on light phenomena and properties (Saleh and Teich [3] and Kumar and Suthar [4] are among the most well-written and updated texts on the PC field and their reading is strongly recommended). More recently, PCs were implemented with plasma media by Hojo and Mase [5], where they studied the dispersion relation of electromagnetic waves in 1-D plasma PCs in a periodic array composed of alternating thin plasma and dielectric material and concluded that this system can be applied to new plasma-functional devices, such as frequency filters in the millimeter-wave (MMW) range. The theoretical study of the interaction of electromagnetic waves with plasma-dielectric structures was made by solving Maxwell's equations for electromagnetism using a method analogous to Kronig–Penny's problem with a periodic potential in quantum mechanics. The extrinsic magnetized plasma is composed of a homogeneous and controllable plasma medium, such as *n*-GaAs or some noble gas. Qi and Zhang [6] and King *et al.* [7] have demonstrated the extrinsic magnetized plasma PCs, in which the modulation of the dielectric constant of a bulk plasma system is achieved with the use of a spatial varying external magnetic field, and, as a consequence, these structures can present photonic bandgaps. During the past two years, we have studied the light propagation in extrinsic magnetized plasma PCs and reported that the bandgaps in these structures can be managed, adjusted, controlled, and even tuned by several practical ways, such as varying the spatial arrangement, external magnetic field, and different plasma parameters [8]–[13].

On the other hand, deterministic and random modulated dielectric constant multilayers give rise to two new families of photonic structures namely photonic quasicrystals and disordered PCs, respectively (see [14]–[17], and the references therein). While studying these photonic structures, particularly the disordered ones, many physical phenomena have been observed, including Anderson localization [14], necklace states [18], colocalization of photon and phonon [19], decay in the oscillation of the average light transmission as a function of the sample length [20], control of average light transmission as a function of disorder [21], among others. The last mentioned physical phenomena in a 1-D random photonic system was proposed by Moretti and Scotognella [22], which developed the theoretical foundation of understanding that the average transmission of a random photonic structure can be controlled by the choice of the standard deviation of the layer thickness. Following the same idea, Nayak *et al.* [9] estimated the average transmission of the photonic bandgap below the plasma frequency in a Gaussian-distributed randomly layered extrinsic bulk magnetized plasma system. The main goal of that study was to achieve efficient photonic structures with low transmission in a wide range of the spectrum. Since the extrinsic plasma PCs have also exhibited another bandgap above the plasma frequency, in a recent report, Nayak *et al.* [13] concluded that this new bandgap is robust against the layer position and becomes wider as the randomness in layer thickness increases. They considered a set of the quasiperiodic

Manuscript received October 30, 2019; revised April 3, 2020; accepted May 9, 2020. Date of publication May 22, 2020; date of current version June 10, 2020. The work of Carlos H. Costa was supported in part by the Brazilian Research Agencies CNPq under Grant 429299/2016-8 and in part by FUNCAP under Grant BP3-0139-00177.01.00/18. The review of this article was arranged by Senior Editor S. J. Gitomer. *(Corresponding author: Chittaranjan Nayak.)*

Chittaranjan Nayak and Kanaparthi V. Phani Kumar are with the Department of Electronics and Communication Engineering, SRM Institute of Science and Technology, Chennai 603202, India (e-mail: 83chittaranjan@gmail.com; phanikuk@srmist.edu.in).

Carlos H. Costa is with the Universidade Federal do Ceará at Campus de Russas, Russas 62900-000, Brazil (e-mail: carloshumberto@ufc.br).

Color versions of one or more of the figures in this article are available online at http://ieeexplore.ieee.org.

Digital Object Identifier 10.1109/TPS.2020.2994243

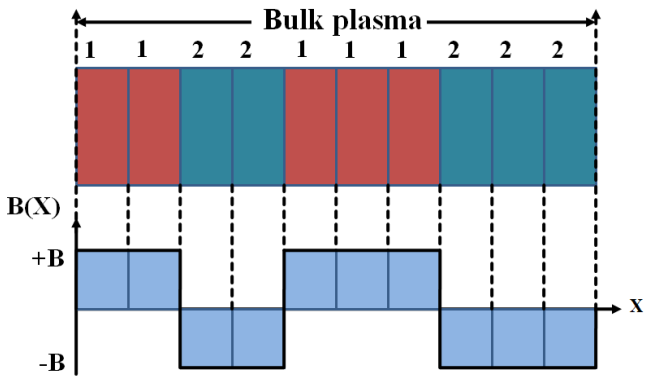

Fig. 1. (Color online) Schematic of a random in layer position extrinsic plasma multilayer with $N = 10$ layers.

arrangement, including Fibonacci, Thue-Morse, double-period [23], and Octonacci [11], [24] of an extrinsic magnetized plasma multilayer. However, the deterministic rule of the used quasiperiodic sequences specifying the layer count, type, and their location regardless they are not able to quantify the order of robustness against the layer position handled by such superlattices. Therefore, it is interesting to know the order of change in layer position and their count that does not have any impact on the bandgap. One of the ways to verify this is by simulating the transmission spectra of the possible permutations [25] of the abovementioned photonic structures with different probabilities. In this article, we have investigated the histogram of average transmission of possible permutations for the entire range of probability of occurrence to quantify the order of change in layer position and the count that can be sustained by the bandgap. Furthermore, as this bandgap is strongly dependent on the external magnetic field and energy density of the magnetized plasma, therefore, an investigation was performed over a range of magnitude of external magnetic field and plasma parameters.

This article is organized as follows. The transfer-matrix method for a random layered thickness extrinsic magnetized plasma multilayer, the considered random multilayer and the dispersion equation of magnetized plasma for normal incidence are deduced and presented in Section II. In Section III, we present and discuss the numerical results for the influence of the probability of occurrence of the layer on the average light transmittance spectra for normal incidence in Sections III-A and III-B. The dependence of the average light transmittance spectra on the external magnetic field and energy density are investigated in Sections III-C and III-D, respectively. Finally, our conclusions are summarized in Section IV.

II. General Theory

In Fig. 1, we present a finite homogeneous bulk plasma system surrounded by air along with some possible profile of the spatial variation of the external magnetic field $B(x)$ (the labels 1 and 2 refer to two different slabs with their respective optical properties and thicknesses). It will be explained later, but it is important to note that, for a given region, the magnetic field is considered constant. The physical properties of the plasma medium can be well described by the free-electron model, whose electromagnetic response, as a function of the angular frequency ω and the external magnetic field B, is given by Drude's permittivity [26], that is

$$\varepsilon_{MP}(\omega, B) = 1 - \left[\frac{\omega_p^2}{\omega^2\left(1 - i\frac{\gamma}{\omega} \mp \frac{\omega_l}{\omega}\right)}\right] \tag{1}$$

where $\omega_p = \left(n_e e^2/m_e\varepsilon_0\right)^{1/2}$ is the plasma frequency, $\omega_l = eB/m_e$ is the gyro-magnetic frequency, γ is the effective collision frequency, n_e being the electron concentration, and e, m_e, and B denote elementary electron charge, electron mass, and magnetic field intensity, respectively. The –(+) sign in ω_l refer to the positive(negative) magnetic field and is called the right(left)-hand polarization, RHP (LHP). According to (1), taking positive and negative values for the magnetic field will produce two different media (labeled as 1 and 2 in Fig. 1) with their respective dielectric permittivities ε_1 and ε_2.

The 1-D random in position magnetic field influences the bulk plasma system $B = B(x)$ has the form

$$B(x) = \begin{cases} B_1, & 0 \le x \le d \\ B_2, & d \le x \le 2d \\ B_3, & 2d \le x \le 3d \\ \quad\vdots & \\ B_{N-1}, & (N-2)d \le x \le (N-1)d \\ B_N, & (N-1) \le x \le Nd \end{cases} \tag{2}$$

where B_j $(j = 1, 2, 3, \ldots, N)$ represents the magnitude of the $B(x)$ for the region between $(j-1)d \le x \le jd$ and are considered constant inside every region, j is the number of the region where the magnetic field B_j is applied, $d_j = d$ is the width of each region (here, we consider that all regions have the same width). Therefore, the system has a finite width and is always equal to Nd.

As we aim to design a disordered multilayered photonic system having two materials with random layer position, the value of B_j is either B or $-B$, and their regions are determined by the probability of occurrence $p(B)$ and $p(-B)$, whose sum is always equal to one, that is, $p(B) + p(-B) = 1$. In order to obtain a random sequence, we use a random number generator function to choose between B (or RHP) and $-B$ (or LHP) and create a chain with N of these two letters, considering a given probability of B. With such 1-D spatially random in position magnetic field applied to the bulk plasma system, the system behaves like a two material finite random in position photonic multilayer. The regions $x < 0$ and $x > Nd$ are the incident and emergent media (considered as being air in this work), respectively, and where the applied magnetic field is equal to zero.

The transmittance T of a multilayered random in layer position extrinsic plasma multilayer system with N slabs is given by $T = 1/|M_{11}|^2$ [27]. To calculate the element M_{11} for the random system having specific probability with two mutually exclusive events B and $-B$, one must obtain the transfer-matrix M for the light propagation through the system,

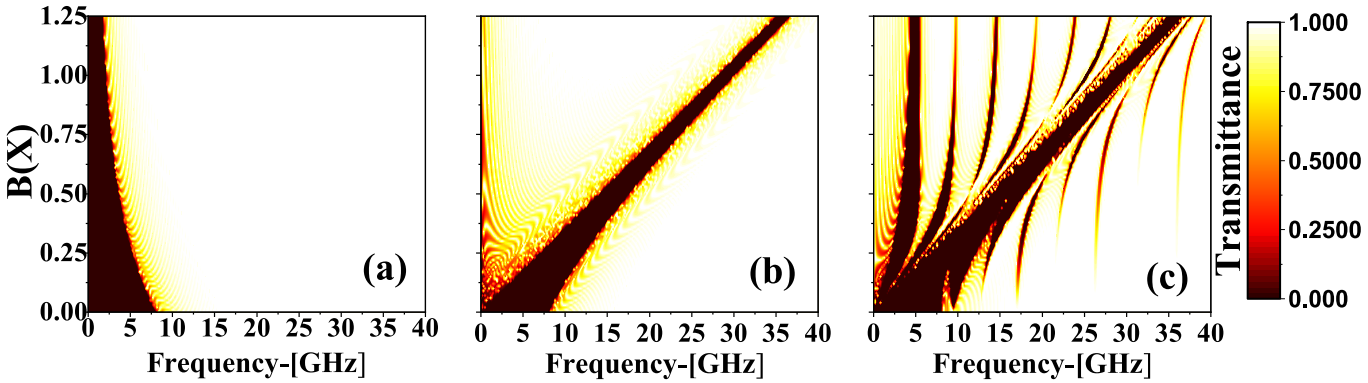

Fig. 2. (Color online) Transmittance, as a function of the frequency and the external applied magnetic field, for (a) LHP bulk plasma, (b) RHP bulk plasma, and (c) periodic extrinsic magnetized plasma multilayer, having $n_e = 8 \times 10^{17}$ m^{-3}.

and it is given by

$$M = \begin{bmatrix} M_{11} & M_{12} \\ M_{21} & M_{22} \end{bmatrix} = D_0^{-1} \left[\prod_{j=1}^{N} D_{j,\alpha} P_{j,\alpha} D_{j,\alpha}^{-1} \right] D_0 \quad (3)$$

where M_{12}, M_{21}, and M_{22} are the other matrix elements. Here, $\alpha = B$ or $-B$, $P_{j,B}(P_{j,-B})$ and $D_{j,B}(D_{j,-B})$ stand for propagation matrix and dynamic matrix of the jth region having thickness d_j and permittivity $\varepsilon_{j,B}(\varepsilon_{j,-B})$, respectively. D_0 is the dynamic matrix for air. For normal incidence, $P_{j,\alpha}$ and $D_{j,\alpha}$ are expressed as [15]

$$P_{j,\alpha} = \begin{bmatrix} e^{i\omega\sqrt{\varepsilon_{j,\alpha}}d_j/c} & 0 \\ 0 & e^{-i\omega\sqrt{\varepsilon_{j,\alpha}}d_j/c} \end{bmatrix} \quad (4)$$

and

$$D_{j,\alpha} = \begin{bmatrix} 1 & 1 \\ \sqrt{\varepsilon_{j,\alpha}} & \sqrt{\varepsilon_{j,\alpha}} \end{bmatrix} \quad (5)$$

where c is the speed of light in vacuum.

III. Numerical Results and Discussion

As previously discussed, the system used in the numerical simulations is the magnetized bulk plasma which is influenced and designed by an 1-D spatially varying external magnetic field according to (2) and is surrounded by air. Only the normal incidence case is considered throughout this entire manuscript, and the direction of light incidence is from left to right. The 1-D spatially periodic magnetic field has $N = 32$, and the thickness of each layer is taken to be 15 mm, so that the total width of the bulk plasma Nd is 48 cm. We consider the frequency range $0 < f < 40$ GHz with several devices such as radio astronomy [28], remote sensing [29], and telecommunications [30] that work on this frequency range called extremely high frequency (EHF). Besides, another very important application relies on the treatment of some human diseases called MMW therapy or EHF therapy [31]. The range for the intensity of the external magnetic field is $0 < B(x) < 1.25$ T, which corresponds to the interested transmittance regions [13]. In the next subsections, we investigate how the light wave transmission coefficient in a extrinsic magnetized bulk plasma PC evolves considering: in Section III-A, a continuous and the periodic external magnetic field; in Section III-B, a random external magnetic field having different probabilities of occurrence; in Section III-C, a random external magnetic field for different values of magnetic fields; and in Section III-D, a random external magnetic field for different values of electron densities.

TABLE I

Bandwidths of the Gaps, in GHz, for LHP, RHP, and Periodic EMPM for Different Values of B_{EXT} (See Fig. 2)

B_{ext} (T)	LHP	RHP	Periodic	
			Bandgap 1	Bandgap 2
0	0 – 8	0 – 8	0 – 8	–
0.25	0 – 5.2	7.04 – 12.24	2.17 – 4.13	6.77 – 12.16
0.5	0 – 3.68	14.01 – 17.61	3.29 – 5.37	13.88 – 17.99
0.75	0 – 2.64	21.04 – 23.68	3.84 – 5.49	20.99 – 23.31
1	0 – 2.09	27.97 – 30.15	4.13 – 5.45	27.97 – 30.15
1.25	0 – 1.68	35.04 – 36.72	4.33 – 5.37	35.09 – 36.80

A. Transmission in a Bulk Plasma System Influenced by a Continuous and Periodic External Magnetic Field

Here, we discuss the dispersive properties of magnetized bulk plasma, influenced by a positive, negative, and periodically arranged external magnetic field. In Fig. 2, the dependence of the transmittance on both frequency and magnetic field is plotted for a LHP, in Fig. 2(a), a RHP, in Fig. 2(b) and an 1-D spatially periodic magnetic field, in Fig. 2(c). The parameters of the magnetized plasma used here are $\gamma = 4\pi \times 10^2$ GHz and $n_e = 8 \times 10^{17}$ m^{-3}.

Fig. 2 shows that the unpolarized bulk plasma, $B(x) = 0$ T case, behaves as a high pass filter having the cutoff frequency around 8 GHz. When $B(x)$ increases, from Fig. 2(a) and (b) one can see that the spectra are polarization-dependent and the bandgap width decreases as the intensity of the magnetic field increases. For LHP (RHP), this bandgap is red (blue) shifted and is this due to the changes in the dielectric of the magnetized plasma material (see [12] for a detailed discussion). If the external magnetic field is 1-D and spatially periodic, Fig. 2(c) shows that the transmission spectrum has a large number of tiny bandgaps including the primary bandgaps appeared in the case of RHP as well as LHP bulk plasma with some measurable modifications [13]. As is shown in Fig. 2,

TABLE II

POLARIZATION OF LAYERS FOR THE SEVEN RANDOM IN LAYER POSITION EMPM MULTILAYERS CONSIDERING THREE DIFFERENT PROBABILITIES

	1	2	3	4	5	6	7	8	9	10	11	12	13	14	15	16	17	18	19	20	21	22	23	24	25	26	27	28	29	30	31	32
																$p(B) = 0.25$																
I	L	L	R	R	L	L	L	R	L	L	R	L	L	R	L	R	R	R	R	R	R	L	L	L	L	L	L	L	R	L	L	L
II	L	R	L	L	L	R	L	R	R	R	R	L	L	R	L	L	L	R	L	L	L	L	L	L	R	L	R	R	L	L	L	L
III	L	L	R	L	L	L	L	L	R	R	L	L	L	R	L	L	L	L	L	L	L	L	L	R	R	L	R	L	L	R	R	L
IV	L	L	L	R	L	L	L	R	L	L	R	R	L	R	R	R	L	R	L	R	R	L	L	R	L	L	L	R	L	R	L	L
V	L	R	R	L	L	L	R	L	L	L	L	R	R	L	L	L	L	L	L	L	L	L	L	R	L	L	L	L	R	R	L	L
VI	L	L	L	R	R	R	L	L	L	R	L	R	R	L	L	L	L	L	L	R	L	L	L	R	L	L	L	L	L	L	R	R
VII	L	R	L	L	R	L	L	R	L	R	L	R	L	R	L	R	R	L	L	L	L	L	L	L	L	L	R	L	R	L	L	L
																$p(B) = 0.50$																
I	L	R	R	R	L	R	R	L	R	R	L	L	R	R	R	R	R	L	L	L	R	L	R	R	R	R	R	R	R	R	R	R
II	L	L	L	R	R	R	L	L	L	R	R	L	L	R	R	R	R	L	R	L	R	L	R	R	R	L	L	R	L	R	L	L
III	L	R	R	R	R	R	L	L	R	R	R	R	R	R	L	L	L	R	R	L	L	L	L	R	L	R	R	R	L	R	R	L
IV	L	L	L	R	L	L	L	R	L	L	R	L	R	L	R	R	R	R	R	L	L	L	R	L	L	L	R	R	L	R	R	L
V	L	L	L	R	R	L	R	L	L	L	L	L	L	R	R	L	L	R	L	R	L	L	R	R	R	R	R	L	R	L	L	L
VI	R	L	R	L	R	R	R	L	R	R	L	R	L	R	L	R	L	L	L	L	R	L	L	L	R	R	R	R	L	L	R	L
VII	R	L	L	R	L	R	L	L	L	L	L	L	R	R	R	R	R	L	L	R	R	L	L	L	L	L	R	L	R	R	L	L
																$p(B) = 0.75$																
I	R	R	L	R	R	R	R	R	R	L	R	L	R	L	R	R	R	R	R	R	L	R	R	L	L	L	R	R	R	R	R	R
II	R	R	R	R	R	L	L	L	R	R	R	R	R	L	R	R	R	L	R	R	R	R	R	L	R	R	R	R	R	R	L	L
III	R	L	R	R	L	L	R	R	R	L	R	R	R	L	R	R	L	R	R	L	R	R	R	R	L	R	R	R	L	R	L	R
IV	L	R	R	R	R	R	R	R	R	R	R	R	R	R	R	L	R	R	R	L	R	R	R	L	R	R	L	R	R	L	R	L
V	R	R	R	R	R	L	R	R	L	R	R	R	R	R	R	R	R	R	R	R	L	R	L	R	R	R	R	L	R	R	L	R
VI	R	R	R	R	R	L	R	R	L	L	R	R	L	R	L	R	R	R	R	R	R	R	R	R	R	R	L	L	R	R	R	R
VII	R	L	L	R	L	L	R	L	L	R	R	R	R	R	R	R	R	L	L	L	R	R	L	L	R	R	R	R	R	R	L	L

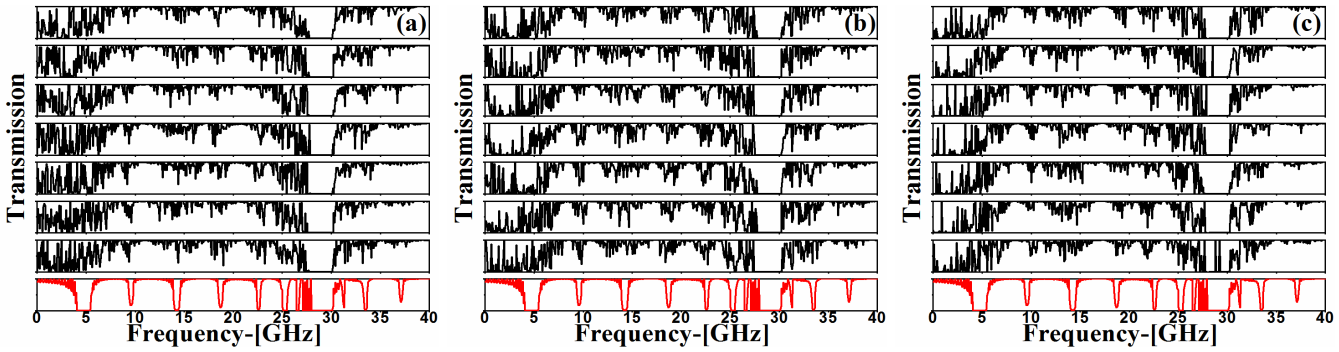

Fig. 3. (Color online) Transmittance versus frequency for seven random extrinsic magnetized plasma structures (black solid lines), with $B(x) = 1$ T. (a) $p(B) = 0.25$. (b) $p(B) = 0.5$. (c) $p(B) = 0.75$. The red solid line in the bottom is the transmission for an 1-D periodic EMPM PC.

at $B(x) = 1$ T, the bandgap regions for the LHP and the RHP magnetized bulk plasma runs from 0 to 2.09 and 27.97 to 30.15 GHz, respectively, whereas the two wider bandgap regions for the periodic extrinsic magnetized bulk plasma runs 4.13–5.45 and 27.97–30.15 GHz. It is noted here that this second main bandgap of the extrinsic magnetized cold plasma is merely following the forbidden gap provided by the RHP bulk plasma. The bandwidths of the bandgaps for LHP, RHP, and periodic extrinsic magnetized plasma media (EMPM) for different values of external magnetic field intensity B_{ext} are summarized and detailed in Table I In this table, the bandgaps 1 and 2 are the two main gaps that emerge in the light transmission spectrum for the periodic structure, being the label 1(2) for the lower(higher) frequency gap.

As was earlier reported by Nayak *et al.* [9], introducing the random in layer thickness, narrow transmission peeks emerged only in the first main bandgap region (4.13–5.45 GHz), while for the second one, such effect was not observed [13]. Moreover, the robustness of the second main bandgap has been predicted in terms of change in layer position, but the level of robustness is unknown. Therefore, the next subsections are dedicated to present some detailed results regarding the robustness of this second bandgap.

B. Transmission for a Random External Magnetic Field Considering Different Probabilities of Occurrence

In the previous subsection, we have calculated the light wave transmission in an extrinsic magnetized plasma for LHP, RHP, and 1-D spatially periodic magnetic field, but now we are interested in to know how the behavior of the bandgap changes with the layers position and their count. To answer this question we calculated the transmittance spectra of the 32 layered photonic structure for five different cases, that is, the probabilities of occurrence of LHP plasma media or B layers $p(B)$ in the random extrinsic photonic 1-D structure are equal to 0, 0.25, 0.5, 0.75, and 1. Here, the parameters of the magnetized plasma are the same as in Section III-A, and the intensity of the external magnetic field is $B(x) = 1$ T. By observing the statistical statement, the cases $p(B) = 0$ and 1 correspond to the RHP and LHP magnetic bulk plasma, respectively, and they were well discussed above. The transmittance for the other three cases is plotted in Fig. 3 (the vertical scale is from 0 to 1 in all plots). For each of the three cases, we have considered seven different types of EMPM ramdomly regenerated according to each probability and the sequences of the layers are presented in Table II, where the letter R(L) represents a RHP(LHP) plasma medium.

TABLE III

BANDWIDTH OF THE ROBUST GAP, IN GHz, IN EMPM FOR DIFFERENT VALUES OF $p(B)$ WITH $B_{\text{EXT}} = 1$ T (SEE FIG. 3)

	$p(B)$		
	0.25	0.5	0.75
Periodic	28 – 30.08	27.97 – 30.08	28.03 – 28.56
I	27.76 – 30.08	28.03 – 30.16	28.56 – 29.92
II	27.68 – 30.08	27.44 – 30.15	27.76 – 30.16
III	27.92 – 30.08	27.76 – 30.15	27.76 – 30.16
IV	27.76 – 30.08	27.76 – 30.15	27.76 – 30.16
V	27.76 – 30.08	27.68 – 30.15	27.84 – 30.16
VI	27.76 – 30.08	27.76 – 30.15	27.84 – 30.16
VII	27.76 – 30.08	27.92 – 30.15	29.28 – 30.28

TABLE IV

BANDWIDTH OF THE ROBUST BANDGAP, IN GHz, IN EMPM FOR DIFFERENT VALUES OF B_{EXT} WITH $p(B) = 0.5$ (SEE FIG. 4)

	$B_{ext} = 0.5$ T	$B_{ext} = 1.25$ T
Periodic	13.71 – 17.96	34.95 – 36.79
I	13.71 – 17.96	34.63 – 36.79
II	13.71 – 18.04	34.79 – 36.79
III	13.79 – 18.04	34.63 – 36.79
IV	13.71 – 18.12	34.63 – 36.79
V	13.87 – 17.96	34.63 – 36.79
VI	13.63 – 17.96	34.79 – 36.79
VII	13.71 – 18.12	34.96 – 36.79

The transmission spectra for the seven random and for the periodic (red solid line in the bottom) EMPM structures having $p(B) = 0.25$ are shown in Fig. 3(a). Here and everywhere else, the transmission plots for all the seven random structures are in black solid lines and they are presented in sequences I–VII, from top to bottom, while the transmission plot for a periodic 1-D EMPM is in red solid line. As shown in Figs. 2(c) and 3(a), for frequencies among 0 and 40 GHz, many bandgaps emerge at several positions for the periodic structure. The first main bandgap and the other tiny bandgaps disappear in all plots due to the presence of randomness in the layer position and their count. The same behavior is also observed in the other two cases $p(B) = 0.5$ and 0.75 displayed in Fig. 3(b) and (c), respectively. However, the second main bandgap, which emerges in the frequency region from 27.97 to 30.15 GHz, is almost unchanged (except for one or two transmission peaks presented only in two random sequences for $p(B) = 0.75$) even considering random arrangements of the LHP|RHP magnetized plasma layers, resulting in a null transmission for this whole frequency range. This is due to the concurrence of the higher dielectric contrast between the RHP and LHP for this frequency range [13], showing to have a stronger influence on the light propagation than the effect of randomness in the layers. This observation can be verified more clearly in Table III, which presents the bandwidth of this robust gap in random 1-D EMPM for the different values of the probabilities $p(B)$ investigated and also considering $B_{\text{ext}} = 1$ T.

As explained above, random extrinsic magnetized plasma structures having $p(B) = 0.5$ means that the structures have an equal amount of RHP and LHP plasma layer, but their positions are random. From Fig. 3(b) and Table III, it is noted that, for the seven random structures, an unchanged bandgap region, from 27.97 to 30.15 GHz, always emerges despite the disorder. Remarkably, in Fig. 3(c), where we take $p(B) = 0.75$, some random structures present a few transmission peaks inside the second main bandgap region leading to a splitting of the bandgap into two parts whereas most of the spectra are nearly unchanged in the interested region. Therefore, one can state that the robustness of the extrinsic structure decreases when the amount of LHP magnetized plasma layers in the structures increases. On the other hand, by deeply analyzing Fig. 3(a) and (c), where the percentages of the LHP plasma layers are assumed to be 25% and 75%, respectively, we conclude that the impact of RHP plasma layer is mainly to effect the second main bandgap as compared to the LHP one. In order to confirm these statements, in the next subsections, a study considering different values of the magnetic field was made.

C. Transmission for a Random External Magnetic Field Considering Different Values of the Magnetic Field

Now, we discuss the transmission of light in a bulk plasma system under the influence of a random external magnetic field with different magnitudes. Therefore, in Fig. 4(a) and (b) we display the same as in Fig. 3(b), that is, considering $p(B) = 0.5$, but for $B(x) = 0.5$ T and $B(x) = 1.25$ T, respectively. From Fig. 4(a), it is revealed that the patterns of the bandgaps for the disordered structures having $B(x) = 0.5$ T (black solid lines) are comparable with the periodic one (red solid line), but with few resonant peaks near the lower band edge, specifically for the frequency region below 5 GHz. This is due to the ratio of the dielectric constant of the RHP and LHP plasma layers for this magnetic field. In addition, it is noted here that these resonant peaks do not make the forbidden gap provided by the period structure disappear as occurred for $B(x) = 1$ T, shown in Fig. 3(b). Increasing the magnetic field intensity, from Fig. 4(b), it is observed that such resonant peaks do not appear anymore and the bandgap for lower frequency vanishes because of the decrease in the slope of the permittivity provided by the RHP plasma layer for higher magnetic field intensity [13]. In Table IV, we present the bandwidth of the robust gap in periodic and random 1-D EMPM for the different values of the external magnetic field intensity B_{ext} investigated and also considering $p(B) = 0.5$.

To study more carefully the influence random external magnetic field with different magnitudes we calculate the transmittance of a random structure for the entire range for the probability of occurrence of the LHP plasma layers $p(B)$ in steps of 0.02. The study was carried out with 2000 different random structures for each case of the probability of occurrence. That means that, for each case of magnetic field intensity, a total of 100 000 random structures were used. Moreover, the histograms, represented by rows in the figures, for the average transmittance of the forbidden bands are plotted for random structures with 50 bins. The results are presented in Fig. 5, where we have considered $n_e = 8 \times 10^{17}$ m^{-3}.

Fig. 5(a) shows the histograms of the average transmittance when the intensity of the external magnetic field is $B(x) = 0.5$ T. The average transmission was calculated for the wider

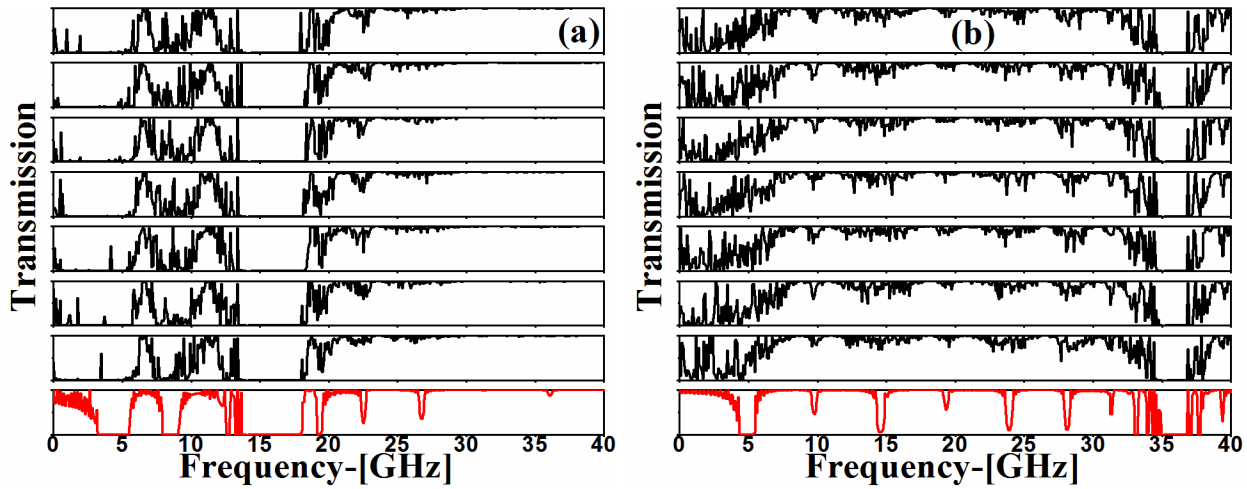

Fig. 4. (Color online) Same as in Fig. 3(b), but for (a) $B(x) = 0.5$ T and (b) $B(x) = 1.25$ T.

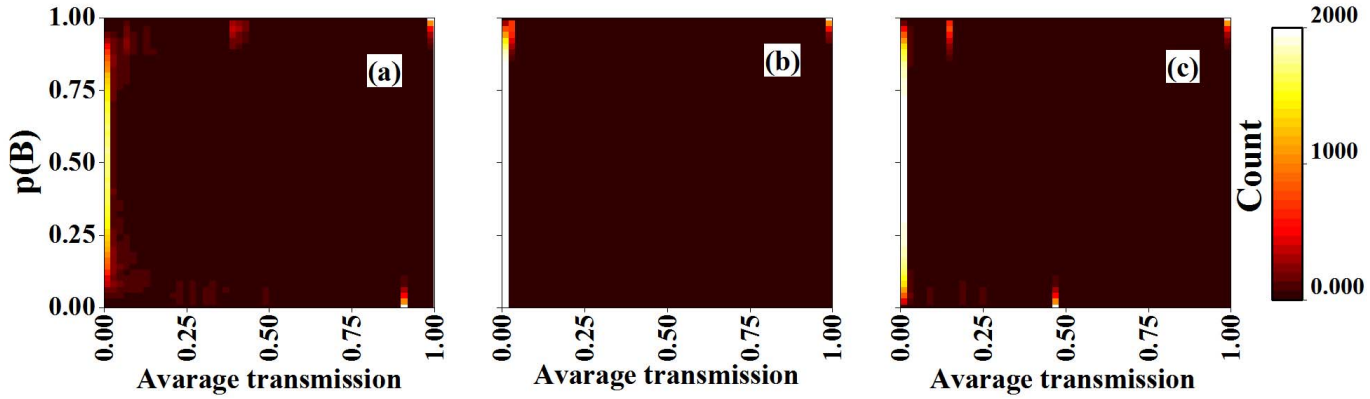

Fig. 5. (Color online) Histogram of the average transmittance of random extrinsic plasma multilayer for the entire range of $p(B)$. (a) $B(x) = 0.5$ T. (b) $B(x) = 1$ T. (c) $B(x) = 1.25$ T.

forbidden band region of the periodic structure which runs, as it can be seen in Table I, from 13.88 to 17.99 GHz [13]. As shown in Fig. 5(a), when $p(B) = 0$, for all 2000 random structures, the area under the transmittance curve within the specified region is 0.9 because of the narrower bandgap from 13.95 to 17.64 GHz provided by the RHP bulk plasma system for this specified magnetic field intensity [see Fig. 2(b)]. With the increase in probability, the count for the specific bin decreases and reaches toward zero which is caused due to the wider bandgap and the presence of narrow peaks within the forbidden region below 5 GHz. This trend is continuing up to $p(B)$ reaches 0.45. After this, the trend of average transmission over the region is reversed and reaches 1, with a count of 2000, when $p(B) = 1$.

In Fig. 5(b), we have the same as in Fig. 5(a), but $B(x) = 1$ T and, therefore, the average transmission is calculated from 27.97 to 30.15 GHz (see Table I). When $p(B) = 0$, for all the 2000 random structures, the area under the transmittance curve within the specified region is insignificant and continues until $p(B)$ reaches 0.76. This means that, up to a specific level, the bandgap provided by the RHP bulk is not modified by the presence of the LHP plasma layer. When the probability of occurrence of LHP plasma layers is higher than 0.76, the trend of the count is decaying, whereas the next bin count is increased up to a certain value and then reaches toward zero. Obviously, this suggests that the forbidden regions of the random structures are not changed evidently with the marginal modification in average transmission. In addition, the nature of the forbidden regions indicates the presence of localization. On the other hand, without any intermediate position in the plot, the average transmission of the reaming structure is directly moving to 1, and their count is increasing as $p(B)$ also increases. Therefore, this suggests that the impact of the LHP plasma layer now dominates the presence of the RHP one. Moreover, it is interesting to note that the count of the bin, which represents the 100% transmission is equal to 2000 in this case.

In Fig. 5(c), we have the case $B(x) = 1.25$ T and the frequency range is from 35.09 to 36.8 GHz (see Table I). Here, a superposition of the effects observed in Fig. 5(a) and (b) is noted. More clearly, we observe that the average transmission is 0.48 for $p(B) = 0$ because of the narrower bandgap as compared to the periodic structure. In addition, as the $p(B)$ increases up to 0.25, we can expect some resonant peaks near the lower limit of the bandgap, but for a higher probability, above 0.75, we find many resonant peaks inside the bandgap

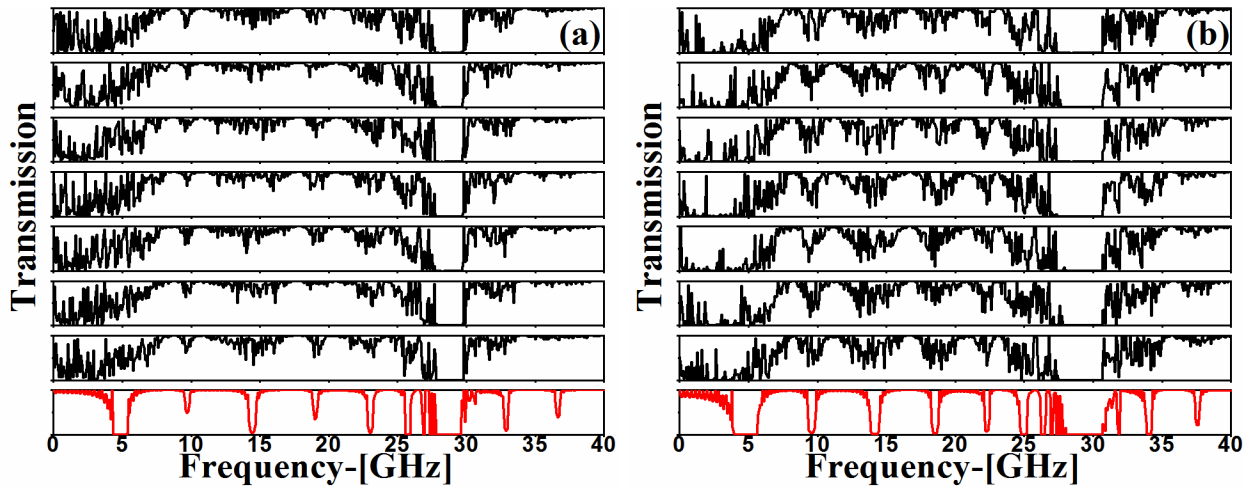

Fig. 6. (Color online) Same as in Fig. 3(b). (a) $n_e = 6 \times 10^{17}$ m^{-3}. (b) $n_e = 10 \times 10^{17}$ m^{-3}.

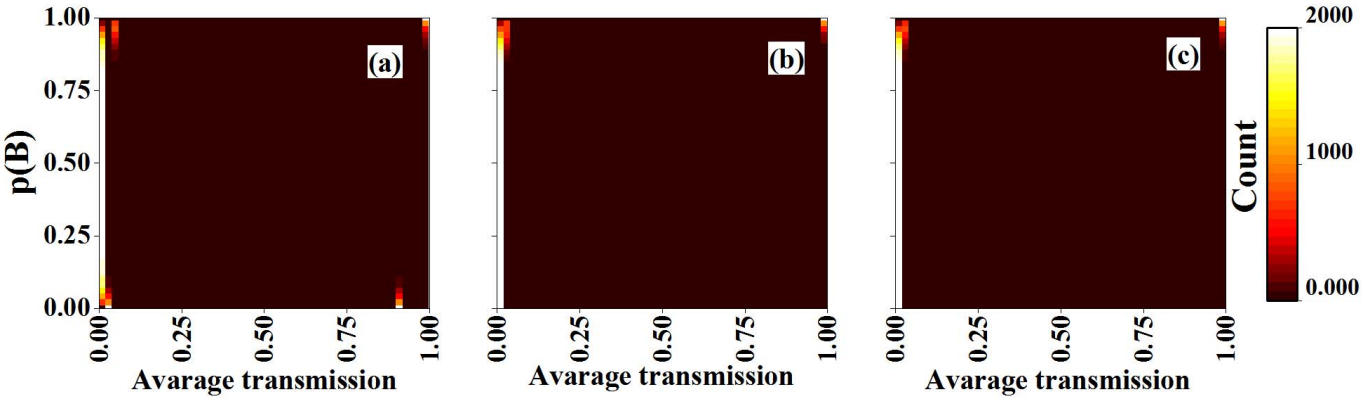

Fig. 7. (Color online) Same as in Fig. 5(b). (a) $n_e = 6 \times 10^{17}$ m^{-3}. (b) $n_e = 8 \times 10^{17}$ m^{-3}. (c) $n_e = 10 \times 10^{17}$ m^{-3}.

region. Moreover, it is noted here that the bin count never reaches to 2000 for any case of probability.

From this article, we can conclude that the robustness feature against layer position and their count in an extrinsic plasma multilayer appears when the magnetic field is around 1 T, when the plasma density is 8×10^{17} m^{-3}. As is expressed in (1), the dielectric constant of magnetized plasma is a function of the plasma parameters such as the plasma density. Therefore, the effect of n_e in a random extrinsic magnetized plasma is examined in the next subsection. We do not present the dependence on the collision frequency γ because its effect is insignificant [32].

D. Transmission for a Random External Magnetic Field Considering Different Values of Electron Density

The transmission spectra of light in a bulk plasma system influenced by a random external magnetic field, having $B_{\text{ext}} = 1$ T and $p(B) = 0.5$, for different electron densities were numerically calculated and they are plotted in Fig. 6. Fig. 6(a) and (b) is same as in Fig. 3(b), but for $n_e = 6 \times 10^{17}$ m^{-3} and $n_e = 10 \times 10^{17}$ m^{-3}, respectively. From Figs. 3(b) and 6, it is observed that the wider forbidden gap regions also are not substantially affected by the position of the LHP or RHP plasma layers in the random extrinsic magnetized plasma photonic lattices. Therefore, one can conclude that, for equal layer count and all the considered range of electron density, the bandgap is robust against the layer position the electron density has no significant effects on this gap. In order to confirm this statement, Table V shows the bandwidth of this robust bandgap in periodic and random 1-D EMPM for different values of n_e investigated and also taking into acount $B_{\text{ext}} = 1$ T and $p(B) = 0.5$.

TABLE V

BANDWIDTH OF THE ROBUST GAP, IN GHz, IN EMPM FOR DIFFERENT VALUES OF n_e WITH $B_{\text{EXT}} = 1$ T AND $p(B) = 0.5$ (SEE FIG. 6)

	$n_e = 6 \times 10^{17}$ m^{-3}	$n_e = 10 \times 10^{17}$ m^{-3}
Periodic	27.81 – 29.58	28.91 – 30.62
I	27.81 – 29.66	27.81 – 30.62
II	27.89 – 29.66	27.89 – 30.62
III	27.81 – 29.66	27.97 – 30.62
IV	27.81 – 29.58	27.97 – 30.62
V	27.81 – 29.66	27.97 – 30.62
VI	27.73 – 29.66	27.97 – 30.62
VII	27.81 – 29.66	27.97 – 30.62

Finally, in order to investigate the influence of random external magnetic field with different electron densities, we calculate the histograms for the average transmittance of the

forbidden bands same as in Fig. 5. Therefore, Fig. 7(b) displays the same as in Fig. 5(b), but in Fig. 7(a) and (c) the electron density are $n_e = 6 \times 10^{17}$ m^{-3} and $n_e = 10 \times 10^{17}$ m^{-3}, respectively. In Fig. 7(a), the average transmission for all the 2000 random structures appears in the first bin when $0.34 < p(B) < 0.66$ whereas for $n_e = 8 \times 10^{17}$ m^{-3} and the $n_e = 10 \times 10^{17}$ m^{-3} the same will appear for the same probability range, which is $0 < p(B) < 0.76$. Therefore, we can conclude that the bandgap of the plasma multilayer is more and more robust against the layer position when the electron density increases.

IV. Conclusion

In summary, the dispersion properties of a random extrinsic magnetized plasma multilayer with different probabilities of occurrence for the LHP magnetic plasma layers $p(B)$ are theoretically studied. By introducing the randomness in layer position of the heterostructure, at $B(x) = 1$ T, up to a certain value of $p(B)$, no localized defect mode appears inside the interested forbidden band from 27.97 to 30.15 GHz, resulting in a zero transmission at the central wavelength of the proposed random 1-D extrinsic PC. A proper choice of the $p(B)$ gives rise to a splitting of the forbidden band, but such events are achieved for higher values of $p(B)$. Also, while decreasing or increasing the intensity of the magnetic field, the robustness of the bandgap for the range of probability is not maintained, specifically in the lower probability regime. However, increasing the electron density makes the bandgap more robust, whereas the collision frequency has a very negligible effect on the bandgap, as is already known. The use of a random layer position to control the properties of a random photonic structure presents many exciting opportunities for all-optical extrinsic switching in the near future.

We hope these very interesting results can encourage and inspire experimental groups to fabricate and experimentally investigate such robust bandgaps in 1-D extrinsic magnetized plasma PCs.

Acknowledgment

Chittaranjan Nayak would like to thank Vice Chancellor, SRM Institute of Science and Technology, Chennai, for his continuous encouragement in this article. The authors would also like to thank Dr. Damodar Panigrahy of the SRM Institute of Science and Technology for useful suggestions and discussions.

References

[1] E. Yablonovitch, "Inhibited spontaneous emission in solid-state physics and electronics," *Phys. Rev. Lett.*, vol. 58, no. 20, pp. 2059–2062, May 1987.

[2] S. John, "Strong localization of photons in certain disordered dielectric superlattices," *Phys. Rev. Lett.*, vol. 58, no. 23, pp. 2486–2489, Jun. 1987.

[3] B. E. A. Saleh and M. C. Teich, *Fundamentals of Photonics, Part II: Photonics*, 3rd ed. San Francisco, CA, USA: Wiley, 2019.

[4] N. Kumar and B. Suthar, *Advances in Photonic Crystals and Devices*, 1st ed. Boca Raton, FL, USA: CRC Press, 2019.

[5] H. Hojo and A. Mase, "Dispersion relation of EM waves in one dimensional plasma photonic crystal," *J. Plasma Fusion Res.*, vol. 80, no. 2, p. 89, Jul. 2004.

[6] L. Qi and X. Zhang, "Band gap characteristics of plasma with periodically varying external magnetic field," *Solid State Commun.*, vol. 151, no. 23, pp. 1838–1841, Dec. 2011.

[7] T.-C. King, C.-C. Yang, P.-H. Hsieh, T.-W. Chang, and C.-J. Wu, "Analysis of tunable photonic band structure in an extrinsic plasma photonic crystal," *Phys. E, Low-Dimensional Syst. Nanostruct.*, vol. 67, pp. 7–11, Mar. 2015.

[8] Z. N. Dehnavi, H. R. Askari, M. Malekshahi, and D. Dorranian, "Investigation of tunable omnidirectional band gap in 1D magnetized full plasma photonic crystals," *Phys. Plasmas*, vol. 24, no. 9, Sep. 2017, Art. no. 093517.

[9] C. Nayak, A. Aghajamali, F. Scotognella, and A. Saha, "Effect of standard deviation, strength of magnetic field and electron density on the photonic band gap of an extrinsic disorder plasma photonic structure," *Opt. Mater.*, vol. 72, pp. 25–30, Oct. 2017.

[10] C. Nayak, A. Aghajamali, and A. Saha, "Double-negative multilayer containing an extrinsic random layer thickness magnetized cold plasma photonic quantum-well defect," *Superlattices Microstruct.*, vol. 111, pp. 248–254, Nov. 2017.

[11] C. Nayak, A. Aghajamali, T. Alamfard, and A. Saha, "Tunable photonic band gaps in an extrinsic octonacci magnetized cold plasma quasicrystal," *Phys. B, Condens. Matter*, vol. 525, pp. 41–45, Nov. 2017.

[12] C. Nayak, A. Aghajamali, and D. P. Patil, "Extrinsic magnetized plasma Fabry–Pérot resonator," *Indian J. Phys.*, vol. 93, no. 3, pp. 401–406, Mar. 2019.

[13] C. Nayak, C. H. Costa, and A. Aghajamali, "Robust photonic bandgaps in quasiperiodic and random extrinsic magnetized plasma," *IEEE Trans. Plasma Sci.*, vol. 47, no. 4, pp. 1726–1733, Apr. 2019.

[14] Y. Lahini *et al.*, "Anderson localization and nonlinearity in one-dimensional disordered photonic lattices," *Phys. Rev. Lett.*, vol. 100, no. 1, Jan. 2008, Art. no. 013906.

[15] A. Arie and N. Voloch, "Periodic, quasi-periodic, and random quadratic nonlinear photonic crystals," *Laser Photon. Rev.*, vol. 4, no. 3, pp. 355–373, 2010.

[16] P. D. García and P. Lodahl, "Physics of quantum light emitters in disordered photonic nanostructures," *Annalen der Physik*, vol. 529, no. 8, Aug. 2017, Art. no. 1600351.

[17] M. Bellingeri, A. Chiasera, I. Kriegel, and F. Scotognella, "Optical properties of periodic, quasi-periodic, and disordered one-dimensional photonic structures," *Opt. Mater.*, vol. 72, pp. 403–421, Oct. 2017.

[18] J. Bertolotti, S. Gottardo, D. S. Wiersma, M. Ghulinyan, and L. Pavesi, "Optical necklace states in Anderson localized 1D systems," *Phys. Rev. Lett.*, vol. 94, no. 11, Mar. 2005, Art. no. 113903.

[19] G. Arregui, N. D. Lanzillotti-Kimura, C. M. Sotomayor-Torres, and P. D. García, "Anderson photon-phonon colocalization in certain random superlattices," *Phys. Rev. Lett.*, vol. 122, no. 4, Feb. 2019, Art. no. 043903.

[20] M. Ghulinyan, "Periodic oscillations in transmission decay of Anderson localized one-dimensional dielectric systems," *Phys. Rev. Lett.*, vol. 99, no. 6, Aug. 2007, Art. no. 063905.

[21] T. Yuan, T. Feng, and Y. Xu, "Manipulation of transmission by engineered one-dimensional disorder in one-dimensional photonic crystals," *Opt. Express*, vol. 27, no. 5, p. 6483, Mar. 2019.

[22] L. Moretti and F. Scotognella, "Control of the average light transmission in one-dimensional photonic structures by tuning the random layer thickness distribution," *Opt. Mater.*, vol. 46, pp. 450–453, Aug. 2015.

[23] C. H. Costa, M. S. Vasconcelos, U. L. Fulco, and E. L. Albuquerque, "Thermal radiation in one-dimensional photonic quasicrystals with graphene," *Opt. Mater.*, vol. 72, pp. 756–764, Oct. 2017.

[24] E. R. Brandão, C. H. Costa, M. S. Vasconcelos, D. H. A. L. Anselmo, and V. D. Mello, "Octonacci photonic quasicrystals," *Opt. Mater.*, vol. 46, pp. 378–383, Aug. 2015.

[25] F. Scotognella, "One-dimensional photonic structure with multilayer random defect," *Opt. Mater.*, vol. 36, no. 2, pp. 380–383, Dec. 2013.

[26] H. G. Booker, *Cold Plasma Waves*, 1st ed. Hingham, MA, USA: Kluwer, 1984.

[27] M. Born and E. Wolf, *Principles of Optics: Electromagnetic Theory of Propagation, Interference and Diffraction of Light*, 7th ed. Cambridge, U.K.: Cambridge Univ. Press, 1999.

[28] C. Sacchi, T. Rossi, M. Murroni, and M. Ruggieri, "Extremely high frequency (EHF) bands for future broadcast satellite services: Opportunities and challenges," *IEEE Trans. Broadcast.*, vol. 65, no. 3, pp. 609–626, Sep. 2019.

[29] R. B. Rustamov, Ed., *Multi-purposeful Application of Geospatial Data*, 1st ed. London, U.K.: IntechOpen, 2018.

[30] T. S. Rappaport *et al.*, "Millimeter wave mobile communications for 5G cellular: It will work!" *IEEE Access*, vol. 1, pp. 335–349, May 2013.
[31] S. D'Agostino *et al.*, "Extremely high frequency electromagnetic fields facilitate electrical signal propagation by increasing transmembrane potassium efflux in an artificial axon model," *Sci. Rep.*, vol. 8, no. 1, p. 9299, Dec. 2018.
[32] H.-F. Zhang, S.-B. Liu, and X.-K. Kong, "Enlarged omnidirectional band gap in one-dimensional plasma photonic crystals with ternary Thue–Morse aperiodic structure," *Phys. B, Condens. Matter*, vol. 410, pp. 244–250, Feb. 2013.

Chittaranjan Nayak received the Ph.D. degree in optoelectronics from the Department of Electrical Engineering, National Institute of Technology Agartala, Jirania, India, in 2017.

He is currently an Assistant Professor with the Department of Electronics and Communication Engineering, SRM Institute of Science and Technology (SRM University), Chennai, India. His current research interests include 1-D photonic multilayers and formation of photonic nanojet for superresolution microscopy.

Carlos H. Costa received the Ph.D. degree in physics from the Department of Physics, Federal University of Rio Grande do Norte, Natal, Brazil, in 2013.

His current research interest includes theoretical investigations of photonic, magnonic, photonic, and polaritonic nanostrutures with periodic, quasiperiodic, and randomic spatial arrangements.

Kanaparthi V. Phani Kumar received the Ph.D. degree in electronics engineering from the Indian Institute of Information Technology, Design and Manufacturing at Kancheepuram, Chennai, India, in 2017.

He is currently working as a Research Assistant Professor with the SRM Institute of Science and Technology, Chennai. His research interests include microwave passive circuits and radio frequency integrated circuit (RFIC).